# ANR POSEIDON D4.1 Proof of Concept - Integration Plan

David Demmer, Jean-Baptiste Doré, Rafik Zayani, Didier Le Ruyet, Pascal Chevalier, Aymen Jaziri, Yoann Corre


anr agence nationale de la recherche

Grant ANR-22-CE25-0015

# Deliverable D4.1
# Proof of Concept - Integration Plan

| | |
|---|---|
| **Deliverable** | 4.1 |
| **Delivery date** | 10/09/2024 |
| **Editor** | CEA-Leti |
| **Authors** | Demmer David, Doré Jean-Baptiste Zayani Rafik - CEA-LETI<br>Le Ruyet Didier, Chevalier Pascal - CNAM<br>Jaziri Aymen, Corre Yoann - SIRADEL |
| **Dissemination** | Public |
| **Keywords** | Factory scenario, Methodology |

**History**

| Version | Date | Modification | Authors |
|---|---|---|---|
| 0.1 | 28/06/24 | First version | Demmer David, Doré Jean-Baptiste |
| 1.0 | 30/07/24 | Integration of comments from june meeting | Demmer David |
| 1.1 | 10/09/24 | Review and comments from partners | Le Ruyet Didier, Chevalier Pascal, Jaziri Aymen |

## Executive summary

The POSEIDON project aims at defining solutions for scalable CF-mMIMO operating in the sub-6GHz frequency bands where the available spectral resources are scarce. In particular, scalable CF-mMIMO architectures must be able to handle i) to support the dramatic increase in wireless traffic demand, which is caused by the exponential growth of connected wireless devices, and ii) the emerging services/applications requiring huge data traffic (e.g., high-quality video calls, holographic communications and Internet of Things/mMTC). Moreover, as an additional target, POSEIDON will propose architectures that may contribute in the roadmap for the necessary transition to greener solutions and infrastructures. With the ICT sector's power consumption increasing exponentially through the different generations of radio mobile networks, a tenfold increase of the power consumption for the wireless access is expected over the next decade. Thus, power consumption is among the critical key performance indicators (KPIs) to be optimized in 6G networks. To this end, POSEIDON will provide solutions to satisfy the expected 6G's requirements with ever-increasingly ubiquitous and reliable wireless connectivity while at the same time steadily addressing the crucial reduction of the ecological impact of cellular infrastructures. The project will focus on lower layers, physical and access, of CF-mMIMO where the consequences of these aforementioned objectives are direct and challenging. WP4 aims at evaluating the benefits of the innovative solutions proposed in WP2 & 3 based on the scenarios and models defined in WP1. A comparison to the reference cellular co-localized mMIMO is the cornerstone of this assessment. Developing a hardware-based proof-of-concept (PoC) of a CF-mMIMO system is challenging and requires a heavy investment in time and budget. Thus, it has been preferred to rely on a software PoC derived from Siradel tool "S_5GConnect". The benefits of POSEIDON techniques will be assessed by considering the deployment constraints of both the access and fronthaul layers as well as the evaluation of end-to-end energy metrics.

## Contents

# 1 Introduction

Poseidon project has been proposed so as to drive a rise in technology readiness level of cell-free massive MIMO (CF-mMIMO) systems with a particular emphasis on the energy efficiency. While WP2 and WP3 focus on the investigation and the design of innovative schemes and techniques dedicated to CF-m-MIMO systems, WP4 aims at evaluating their benefits and gains by comparison with both conventional co-localized mMIMO and state-of-the art CF-mMIMO networks. WP4 objectives can thus be listed as follows:

1. Providing a common and realistic framework for performance evaluation of co-localized and CF MIMO
2. Integrating solutions proposed in WP2 (MAC) and WP3 (PHY)
3. Assessing the interests and benefits of the proposed solutions

In other words, the objective of WP4 is to provide a general framework and a methodology to compare the possible solutions. With this first deliverable, we present a first study considering classical state-of-the-art solutions and the channel predictions obtained for the factory scenario (see deliverable D1.2). Then, a methodology will be generalized and key performance indicators (KPIs) will be defined for forthcoming studies. Besides, a planning of integration and forthcoming studies is detailed in the last section.

# 2 Methodology

## 2.1 Generic system model

The propagation channel is predicted for each possible link for a transmission bandwidth up to $100$ MHz. The propagation channel will be denoted by $\mathbf{H}_k \in \mathbb{C}^{N_r \times N_t}$ where the subscript $k$ is the frequency index, $N_t$ and $N_r$ respectively denote the number of transmit and receive antenna elements (AEs). As one may notice, there is no notion of time. Indeed, the propagation channel is predicted for a given time $t_0$ therefore for sake of simplicity time indices are omitted from now on. Besides for each AE, two polarizations are available (either horizontal (H) and vertical (V) or $\pm 45^\circ$ depending on the scenario).

We will compare the system performance for different deployments of Access Points (APs):

- Cellular: A few APs serve the User Equipments (UEs) in a non-cooperative way (*i.e.* AP selection).
- Distributed : A high density of APs serve the UEs either in a non-cooperative way (*i.e.* AP selection with the 'Stronger 1' mode) or in a cooperative way (*i.e.* joint coherent transmission and/or reception with 'Stronger N' mode where $N \geq 2$ denotes the number of closest cooperative APs). The downlink precoders can be determined in a centralized way (with the full channel state knowledge) or in a local way (with only the AP channel state knowledge).

Let us consider a system composed of a transmitter equipped with $N_t$ transmit antennas and $N_r$ receive antennas. The system supports the transmission of $L$ layers, *i.e.* the number of independent data streams transmitted simultaneously per time/frequency resource. Consider the following orthogonal frequency division multiplexing (OFDM) received baseband signal after postcoding at the k-th subcarrier:

$$\mathbf{y}_k = \mathbf{W}_k \left( \mathbf{H}_k \sqrt{\mathbf{P}_k} \mathbf{F}_k \mathbf{x}_k + \mathbf{n}_k \right), \tag{1}$$

where $\mathbf{y}_k \in \mathbb{C}^{L \times 1}$ and $\mathbf{x}_k \in \mathbb{C}^{L \times 1}$ are the received signal and the transmitted signal, $\mathbf{n}_k \in \mathbb{C}^{L \times 1}$ is the additive white Gaussian noise (*i.e.* $\forall i \ (\mathbf{n}_k)_i \sim \mathbb{C}\mathcal{N}(0, N_0)$), $\mathbf{W}_k \in \mathbb{C}^{L \times N_r}$, $\mathbf{H}_k \in \mathbb{C}^{N_r \times N_t}$, $\mathbf{P}_k \in \mathbb{R}^{N_t \times N_t}$ and $\mathbf{F}_k \in \mathbb{C}^{N_t \times L}$ are respectively the linear combining vector at the Rx side, the propagation channel matrix, the per-antenna amplification gains and the linear precoding vector applied at the Tx side. When uniform inband-power allocation is considered, *i.e.* $\forall k \ P_k = P/N_c$ where $N_c$ is the number of subcarriers. Besides, the per-antenna inband power range can be limited from $-10$ to $30$ dBm. The system model can thus be simplified as follows

$$\mathbf{y}_k = \mathbf{W}_k \left( \sqrt{P/N_c} \mathbf{H}_k \mathbf{F}_k \mathbf{x}_k + \mathbf{n}_k \right). \tag{2}$$

One may define the equivalent channel matrix for the k-th subcarrier $\mathbf{G}_k \triangleq \sqrt{P/N_c} \mathbf{W}_k \mathbf{H}_k \mathbf{F}_k$ ($\mathbf{G}_k \in \mathbb{C}^{L \times L}$) and the Signal to Interference plus Noise Ratio (SINR) for the k-th subcarrier and the l-th layer $\gamma_{k,l}$:

$$\gamma_{k,l} = \frac{\left| (\mathbf{G}_k)_{l,l} \right|^2}{\sum_{i \neq l} \left| (\mathbf{G}_k)_{l,i} \right|^2 + N_0/\sigma_x^2}, \tag{3}$$

where $\sigma_x^2 \triangleq \mathbb{E}_{k,l}[(\mathbf{x}_k)_l (\mathbf{x}_k)_l^*]$.

The corresponding link capacity is the sum of the in-band capacities for each subcarrier and layer:

$$C \triangleq \sum_{l=1}^{L} \sum_{k=1}^{N_c} \min\{\log_2 (1 + \gamma_{k,l}), C_{\max}\} \ \text{[bits/s/Hz]}. \tag{4}$$

One may notice that the capacity per subcarrier is limited to a given value $C_{\max}$ in order to avoid unrealistic high values in low path loss cases. For instance, 'capaMax' can be set to $6$ which corresponds to a $64$-QAM (by neglecting reference signals and coding channel rate). It may be worth noticing that the instantaneous capacity defined in (4) is a random variable which depends on the channel realization, including the deployment of the

transmit and receive antennas over the area, and the noise realization. In practice we define the total Spectral Efficiency (SE) at probability $p$ as follows:

$$\mathrm{SE}_p \triangleq \{x \mid P\left[C = x\right] = p.\} \quad \text{[bits/s/Hz]}. \tag{5}$$

The corresponding sum-rate $R$ is given by:

$$R \triangleq B\eta_{\mathrm{TDD}}.\eta_{\mathrm{CP}}.\eta_{\mathrm{DRMS}}.\mathrm{SE}_p \quad \text{[bits/s]}, \tag{6}$$

where $B$ is the signal bandwidth, $\eta_{\mathrm{CP}}$ the OFDM symbol density (including cyclic prefix), and $\eta_{\mathrm{DRMS}}$ the spectral efficiency loss due to the signalling (e.g demodulation reference signal (DMRS)) and $\eta_{\mathrm{TDD}}$ the loss induced by the time division multiplexing.

It is now possible to define the Energy Efficiency (EE) by taking into account the total power required to obtain a given $\mathrm{SE}_p$ [2],

$$\mathrm{EE}_p \triangleq \frac{\mathrm{SE}_p B}{P_{\mathrm{Tx}} + P_{\mathrm{Rx}}} \quad \text{[bits/J]} \tag{7}$$

with $P_{\mathrm{Tx}}$ and $P_{\mathrm{Rx}}$ the powers required to ensure the transmission at the transmitter and receiver side. The detailed expressions are given below:

$$\begin{aligned} P_{\mathrm{Tx}} &= N_{\mathrm{t}} P \alpha_{PA} + P_{\mathrm{proc}}^{\mathrm{Tx}}, \\ P_{\mathrm{Rx}} &= P_{\mathrm{proc}}^{\mathrm{Rx}}, \end{aligned} \tag{8}$$

with $\alpha_{PA}$ is the power amplifier efficiency (including power input back off) and $P_{\mathrm{proc}}$ the power required for the signal processing part. The latter includes the consumed resources at the RU level, DU level and backhaul use for distributed topologies are considered. This expression (7) is valid for both the downlink and the uplink by adapting the parameter values. Besides, it seems worth noticing that the proposed model here does not take into consideration the amplification at the receiver side (low-noise amplifier).

### 2.2 Single-layer transmission

For the proposed study, only single-layer transmissions (*i.e.* single-user with single datastream) are considered: $L = 1$. The system model equation (2) can be rewritten as follows

$$y_k = \mathbf{w}_k \left( \sqrt{P/N_c} \mathbf{H}_k \mathbf{f}_k x_k + n_k \right) \tag{9}$$

where $\mathbf{w}_k \in \mathbb{C}^{1 \times N_r}$ and $\mathbf{f}_k \in \mathbb{C}^{N_t \times 1}$ are respectively the linear combining vector at the Rx side and the linear precoding vector at the Tx side. In such scenario, there is no inter-layer interference and the corresponding Signal-to-Noise Ratio (SNR) expression and the link capacity become:

$$\begin{aligned} \gamma_k &= \frac{|g_k|^2}{N_0/\sigma_x^2} \\ C &= \sum_{k=1}^{N_c} \min\{\log_2\left(1 + \gamma_k\right), \text{capaMax}\} \quad \text{[bits/s/Hz]} \end{aligned} \tag{10}$$

where $g_k \triangleq \sqrt{P/N_c} \mathbf{w}_k \mathbf{H}_k \mathbf{f}_k$

# 3 Scenario FA1: Indoor factory

## 3.1 System Model

### 3.1.1 Introduction

The deliverable will focus on the "FA1 - Factory - Empty room" scenario depicted in Figure 1. The scenario is fully described in D1.2 but key information is reminded in this section. The environment consists in an indoor room of

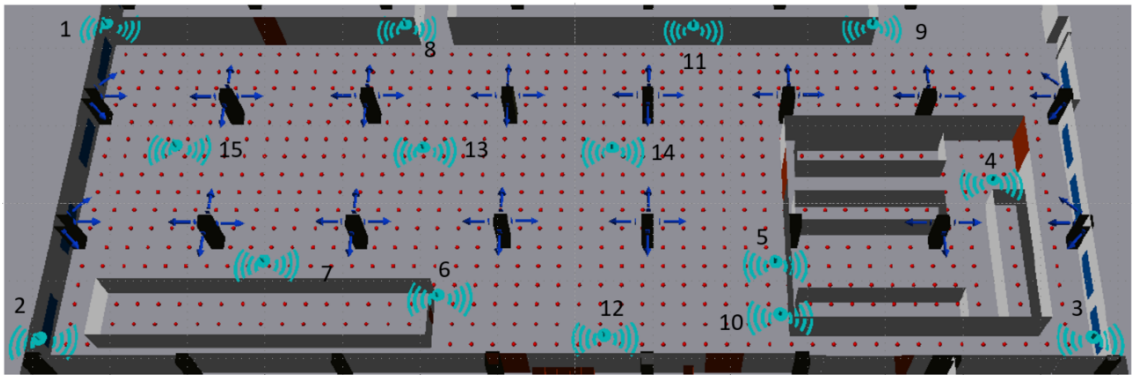


Figure 1: Factory - Empty Room - environment

97m x 36m. $15$ APs equipped with up to $64$ antennas per polarization ($4$ omnidirectional $4 \times 4$ antenna arrays with a square arrangement) are spatially distributed and represented with the light blue signs in Figure 1. In a similar ways, $53$ directive sectors, also consisted of $64$ antennas per polarization ($8 \times 8$ array), are spatially distributed over the room and are depicted with the dark blue arrows in Figure. 1. In addition to the APs, there are $850$ terminal locations ($2$m$\times 2$m grid) represented by the red dots in Figure. 1.

The carrier frequency and the transmission bandwidth for this scenario are respectively $3.7$ GHz and $20$ MHz (*i.e.* $52 \times 360$ kHz). For this first study, we will consider perfect channel state information (CSI) at the transmitter side. Single-layer spatial diversity MIMO schemes will be considered and presented in the following paragraphs.

We will compare the system performance for different AP deployments:

- Cellular: Only APs $14$, $15$ and $4$ serve the UEs in a non-cooperative way (*i.e.* AP selection).
- Distributed : All the APs can serve the UEs in a cooperative way (*i.e.* joint coherent transmission with 'Stronger N' scenarios where $N \geq 2$ denotes the number of closest cooperative APs) or not (*i.e.* AP selection with the 'Stronger 1' scenario).

### 3.1.2 Combiners

**Maximum Ratio Combining** The Maximum Ratio Combining (MRC) cophases each receive signal and weights them by the equivalent channel gain : $(\mathbf{w}_k)_r = \left((\mathbf{H}_k \mathbf{f}_k)_r\right)^*$.

The resulting SNR can then be expressed as follows

$$\begin{aligned} \text{SNR}_k &= \frac{P\left(\sum_{r=0}^{N_r-1} |(\mathbf{H}_k \mathbf{f}_k)_r|^2\right)^2}{N_c N_0 \left(\sum_{r=0}^{N_r-1} |(\mathbf{H}_k \mathbf{f}_k)_r|^2\right)} \\ &= P \sum_{r=0}^{N_r-1} |(\mathbf{H}_k \mathbf{f}_k)_r|^2 / (N_c N_0) \end{aligned} \tag{11}$$

By considering a per-antenna power constraint, *i.e.* $\|\mathbf{f}_k\|_\infty = \max(\mathbf{f}_k)_r = 1$, the SNR bound can be expressed as follows:

$$\text{SNR}_k \leq \frac{P\|\mathbf{H}_k\|_2^2 N_t}{N_c N_o} \tag{12}$$

where $\|\mathbf{A}\|_p \triangleq \sup\left\{\frac{\|Ax\|_p}{\|x\|_p} : \mathbf{A} \in \mathbb{C}^{M\times N}, x \in \mathbb{C}^N\right\}$ is the matrix p-norm operator. The equality is satisfied when all precoder coefficients are unitary.

**Equal Gain Combining** The Equal Gain Combining (EGC) cophases each receive signal and combines them with equal gain: $(\mathbf{w}_k)_r = e^{i\phi_r}$ with $\phi_r = -\angle(\mathbf{H}_k\mathbf{f}_k)_r$. The resulting SNR can then be expressed as follows

$$\text{SNR}_k = P\left(\sum_{r=0}^{N_r-1} |\mathbf{H}_k\mathbf{f}_k|_r\right)^2 / (N_c N_r N_0) \tag{13}$$

By considering a per-antenna power constraint, *i.e.* $\|\mathbf{f}_k\|_\infty = 1$, the SNR bound can be expressed as follows:

$$\text{SNR}_k \leq \frac{P\|\mathbf{H}_k\|_1^2 N_t^2}{N_c N_r N_o} \tag{14}$$

### 3.1.3 Precoders

The APs are likely to exhibit distinct large scale fadings coefficients to given UE. Therefore, per-antenna peak power constraints are required to handle the limited range of each power amplifiers [1].

**Equal Gain Transmission** How to design the precoder and combiner to maximize the receive energy for a constrained transmit energy? Equal Transmission Gain (EGT), combined with either EGC or MRC, can provide full diversity order over memoryless i.i.d. MIMO Rayleigh channels [3]. EGT beamformer weights each transmit signal with an unitary gain $|(\mathbf{f}_k)_l| = e^{i\theta_l}$. The design of the beamformer vectors, *i.e.* the vector $\theta = [\theta_0\ \theta_1\ \ldots\ \theta_{N_t-1}]^T$ of phases to apply on each transmit signal, depends on the combining technique.

With EGC, the optimal EGT corresponds to the maximization of the $\ell^1$-norm of $\mathbf{H}_k e^{i\theta}$ :

$$\theta = \arg\max \left\|\mathbf{H}_k e^{i\theta}\right\|_1 \tag{15}$$

With MRC, the optimal EGT corresponds to the maximization of the $\ell^2$-norm (Euclidean distance) of $\mathbf{H}_k e^{i\theta}$:

$$\theta = \arg\max \left\|\mathbf{H}_k e^{i\theta}\right\|_2 \tag{16}$$

In practice, it is possible to reduce the number of degrees of freedom by setting $\theta_0 = 0$. For $N_t = 2$, determining the optimal EGT can be found by testing possible values for the layer-2 precoding phase. For $N_t \geq 2$, the EGT precoder is not implemented.

**Singular Value Decomposition** It is possible to build a precoding scheme based on the Singular Value Decomposition (SVD). Indeed, for any matrix $\mathbf{H}_k \in \mathbb{C}^{N_r\times N_t}$, it exists a factorization $\mathbf{H_k} = \mathbf{U}_k\mathbf{\Sigma}_k\mathbf{V}_k^H$ where $\mathbf{U}_k \in \mathbb{C}^{N_r\times N_r}$ and $\mathbf{V}_k \in \mathbb{C}^{N_t\times N_t}$ are complex unitary matrices and $\mathbf{\Sigma} \in \mathbb{R}^{N_r\times N_t}$ is a diagonal matrix. The number of non-null singular values corresponds to the rank of $\mathbf{H}_k$ : $\text{rank}\{\mathbf{H}_k\} \leq \min(N_t, N_r)$.

The optimal SVD is the solution of the following optimization problem

$$\alpha = \arg\max \left\{ \left\| \mathbf{H}_k \frac{\sum_{i=0}^{\text{rank}\{\mathbf{H}_k\}-1} \alpha_i \left(\mathbf{V}_k^H\right)_i}{\left\|\sum_{i=0}^{\text{rank}\{\mathbf{H}_k\}-1} \alpha_i \left(\mathbf{V}_k^H\right)_i\right\|_\infty} \right\|_p : \|\alpha\|_2 = 1 \right\}, \tag{17}$$

where $p = 1$ for EGC combiner and $p = 2$ for MRC combiner.

By denoting $\mathbf{f}_{p,k} = \sum_{i=0}^{\mathrm{rank}\{\mathbf{H}_k\}-1} (\alpha_p)_i \left(\mathbf{V}_k^H\right)_i / \left\| \sum_{i=0}^{\mathrm{rank}\{\mathbf{H}_k\}-1} \alpha_i \left(\mathbf{V}_k^H\right)_i \right\|_\infty$ where $\alpha_p$ are the optimal coefficient with respect to the p-norm, the resulting SNR can be expressed as (13) and (11) respectively for EGC and MRC combiners.

SVD precoders also admit (14) and (12) as theoretical bounds. However unlike EGT, it is not possible to equal the bounds because $\|\mathbf{f}_{p,k}\|_2 < 1$. Nonetheless, it is possible to determine the optimal SVD precoder when $\mathrm{rank}\{\mathbf{H}_k\} \leq 2$ which makes it easier to implement than the EGT precoding scheme.

### 3.2 Power and Capacity Maps

First, we will provide some evaluations of rx power maps with Figure 2 and Figure 3. The rx power maps associated to the two polarizations (H and V) are depicted along side the two cross-polar coverage for omni AEs. Link obstructions caused by the indoor pylons and strong attenuation occurring during propagation through walls are clearly noticeable. In particular, the room at the right side of the factory does not receive much power when the AP is outside of this room (Figure 2). However, when the AP is inside, it also illuminates outside when radio paths go through doors and windows. Besides, one can observe that both H and V propagations are rather similar and the cross-polar isolation looks greater than $30$ dB.

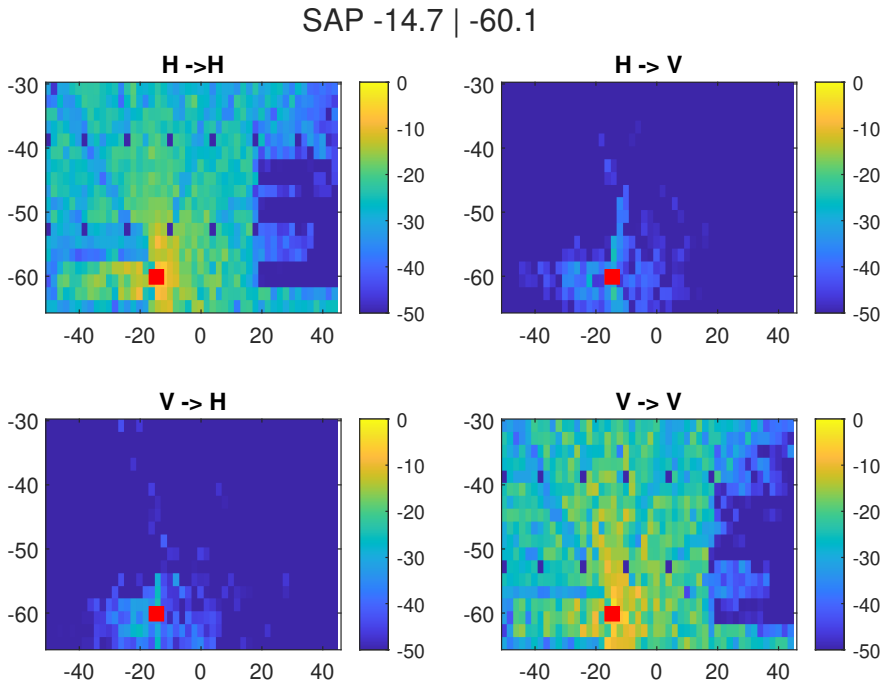


Figure 2: Rx power map [dBm] for omni AP $6$ with a total transmit power $P = 0$ dBm where the $850$ terminal locations $(x, y)$.

We can now evaluate the DL capacity depending on AP deployment scenarios: 'Cellular' (Ap selection among $3$ possible APs), 'Stronger 1' (AP selection among all the $15$ APs), 'Stronger 3' (joint-transmission between $3$ cooperative APs, selection based on total channel strength) and 'Stronger 15' (joint transmission between the $15$ possible APs). For this evaluation, the channel is assumed perfectly known at the transmitter side and the derivation of the precoding coefficients is centralized. The complementary cumulative density function (CCDF) results are depicted in Figure 4 for maps and in Figure 5. One can easily observe the main interest of coherent joint-transmission: to make the spectral efficiency more uniform in the covered area. Indeed, with AP selection scenarios ('Cellular' and 'Stronger 1'), the best-served users are the closest to the serving APs. Increasing the number of serving AP reduces the average distance between UE and AP and thus enhances the minimum capacity. However, there is always a capacity difference between the closest UE to AP and the others. Considering joint-transmission tends to attenuate this difference, especially when several APs are visible in LOS which is the case for most tested locations. However, for UEs located in the room at the right side of the factory, there is only one AP in LOS. Consequently, there is no gain with joint transmission because other APs does not illuminate enough this closed room.

Looking at capacity CCDFs with Figure 5 allows us to better compare the different scenarios. The difference between 'Cellular' and 'Stronger 1' appears clearly once again. The cooperative scenarios ('Stronger 3' and 'Stronger

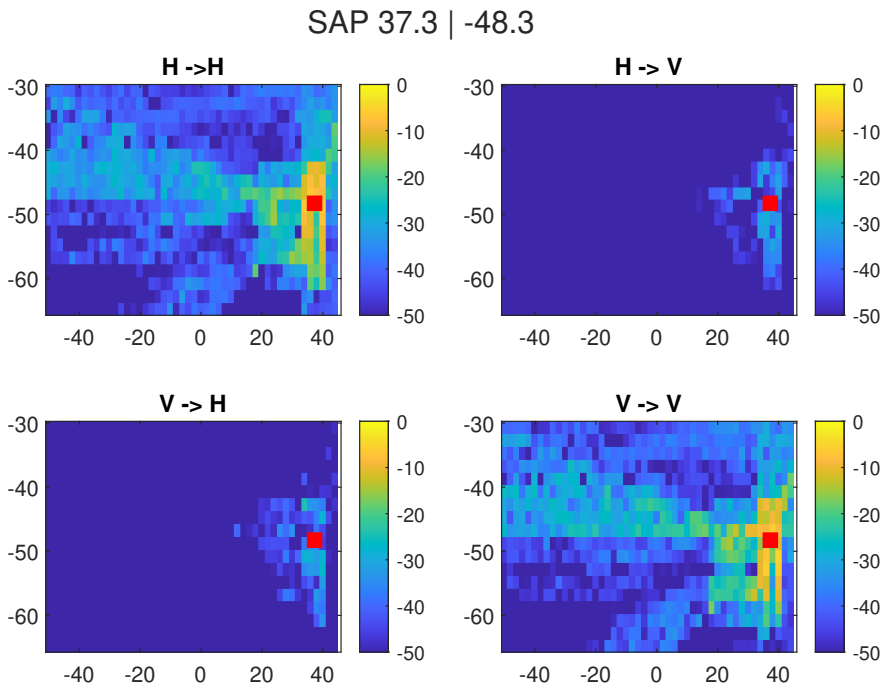


Figure 3: Rx power map [dBm] for omni AP $4$ with a total transmit power $P = 0$ dBm

15') improve the performance with respect to 'Stronger 1' especially for the $90\%$ worst-served users as aforementioned.

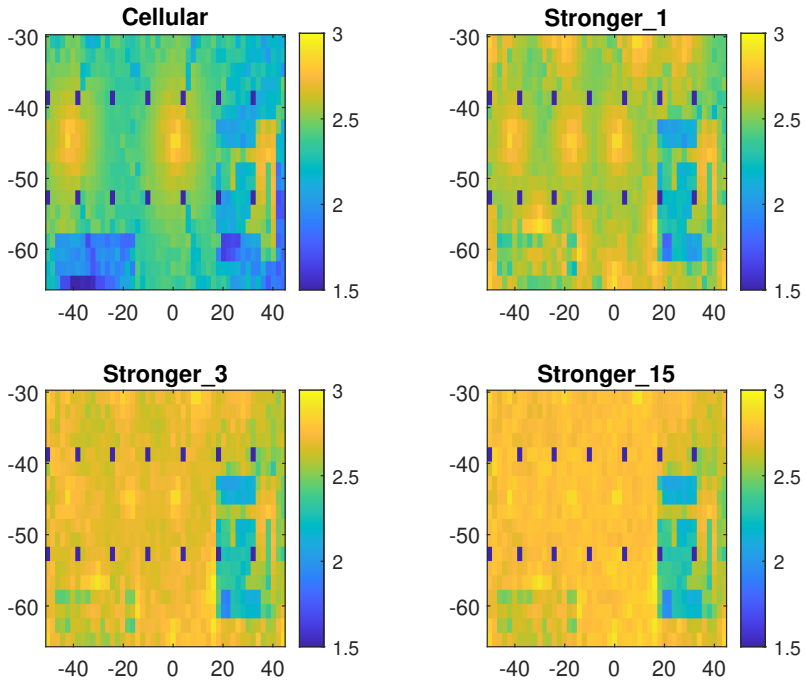


Figure 4: DL capacity map [bits/s/Hz] ($P = 10$ dBm, $N_t = 4$, $N_r = 2$, $50°$ thermal noise $N_0 = -88$ dBm/RB, EGT/MRC, no maximum capacity)

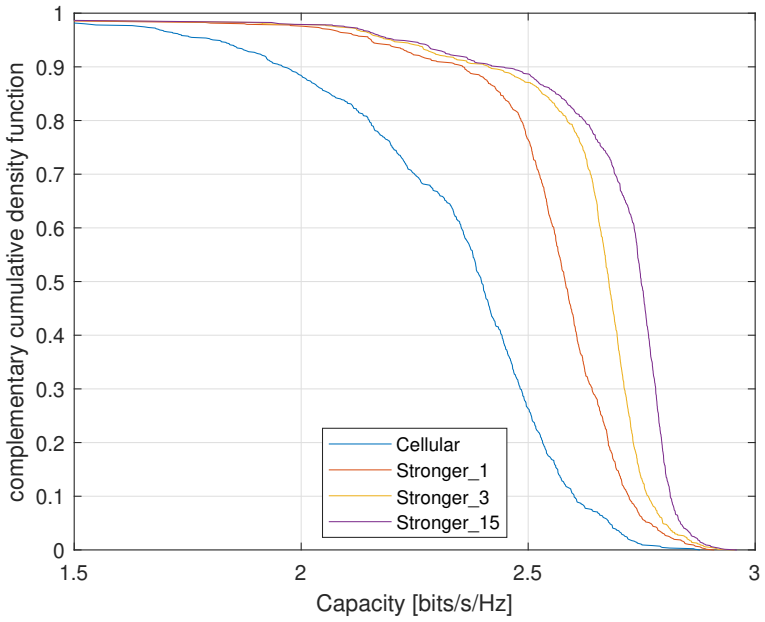


Figure 5: DL capacity CCDF ($P = 10$ dBm, $N_t = 4$, $N_r = 2$, $50°$ thermal noise $N_0 = -88$ dBm/RB, EGT/MRC)

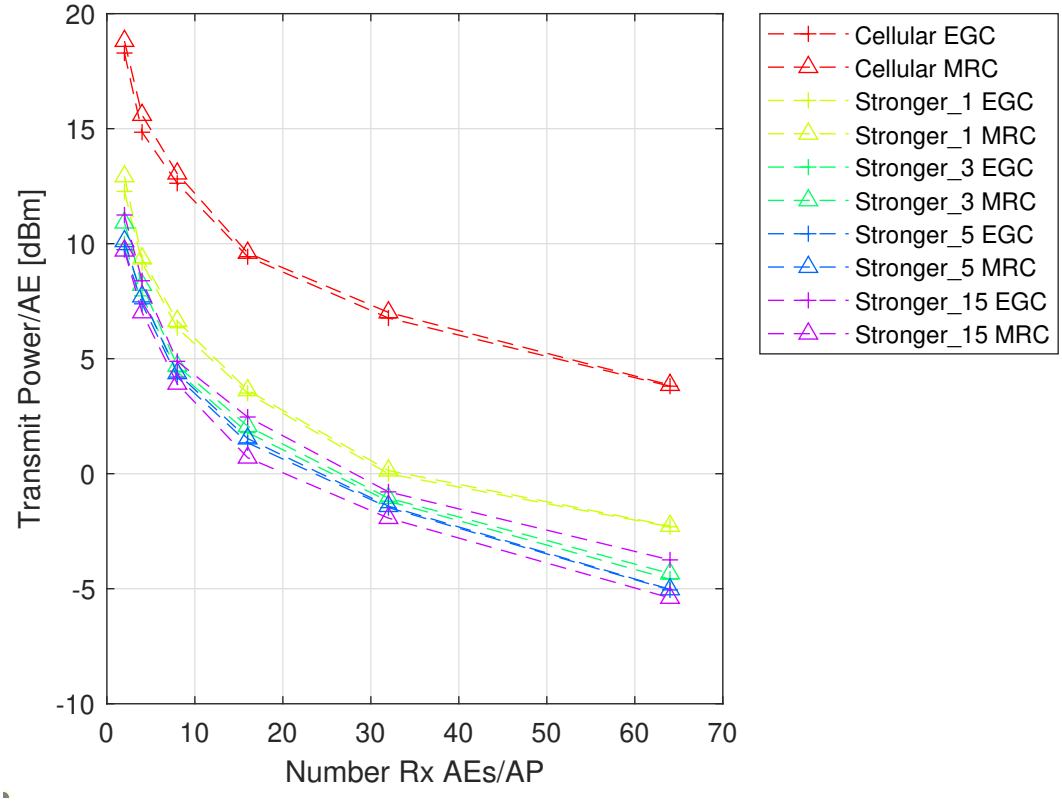


Figure 6: Theoretical bounds of transmitted power per AE required to achieve $SE_{50\%}$ = 2.5 bits/s/Hz (Uplink, $N_t = 2$, H-polar only, $N_0 = -88$ dBm/RB)

### 3.3 Uplink $N_t = 2$

We first evaluate the theoretical performance predicted by relations (14) and (12) and the results are depicted in Figure 6.

For this evaluation, the number of Tx AEs is fixed to $2$. The theoretical performance of the two combiners are highly similar for most deployment scenarios. On the one hand, the EGC combiner slightly outperforms the MRC for AP selection scenario ('Cellular' or 'Stronger 1') when low number of Rx AEs are considered. On the other hand for the full cooperation scenario ('Stronger 15'), the MRC provides an appreciable performance gain. This result is not surprising because with full cooperation, the APs may receive weak signals and thus the MRC combiner avoid noise enhancement. According to these results, the best deployment scenario in terms of spectral efficiency is the cooperation of at least $3$ Rx APs with the highest number of Rx AEs possible. However, when more than $3$ receiving APs are considered the gain is very limited. Therefore, it is likely that an optimal number of receiving sites would appear when the cost of inter-AP cooperation (backhaul use) is taken into account.

The achievable performance for EGT and SVD precoders are given in Figure 7. In Figure 7 (top), the performance of EGT and SVD precoders are compared to the theoretical bound (same as depicted in Figure 6) for MRC combiner. The achievable performance of both precoders are very similar the to theoretical limit. The Figure 7 (bottom) represents the results with EGC combiner. In that case, there is a difference between theoretical and practical performance. The performance gap is limited for AP selection scenarios ('Cellular' and 'Stronger 1'). However it enlarges wit the number of cooperating APs. The achieved performance with full cooperation even becomes worst that 'Stronger 1' scenario. The best deployment scenario looks to be the cooperation of $5$ APs. In general, both EGT and SVD precoders achieve the same performance. The performance difference is mainly due to the

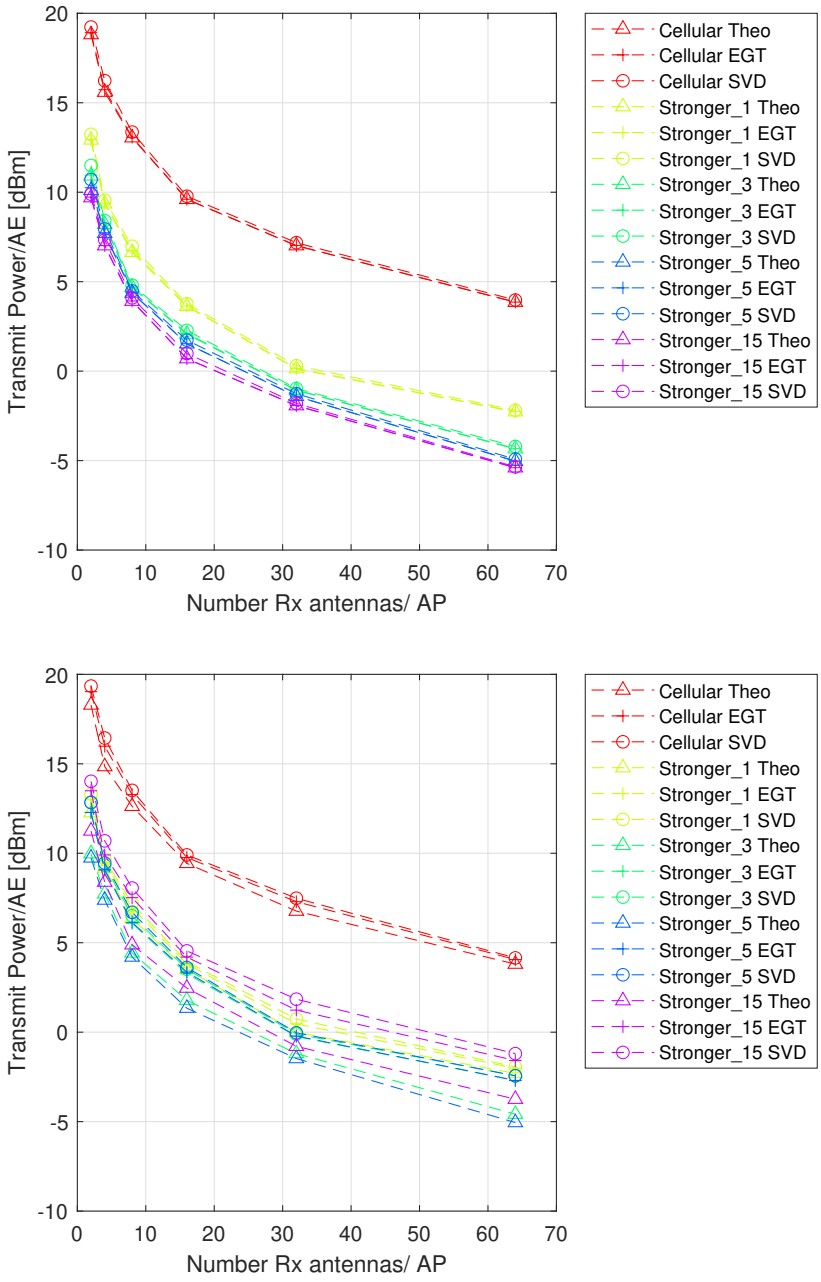


Figure 7: Evaluation of the transmitted power per AE required to achieve $SE_{50\%}$ = 2.5 bits/s/Hz for EGT and SVD precoding schemes with MRC (top) and EGC (bottom) combiners (Uplink, $N_t = 2$, H-polar only, $N_0 = -88$ dBm/RB)

choice of combiner, either EGC or MRC. Indeed, AP cooperation with MRC combiner slightly outperforms the other considered scenarios.

Increasing the number of Rx antennas helps to reduce the required transmit power while satisfying the capacity constraint. Therefore, the higher number of RX antennas, the better in terms of EE. Figure 8 gives the evaluation of the EE for MRC (top) and RGC (bottom) combiners.

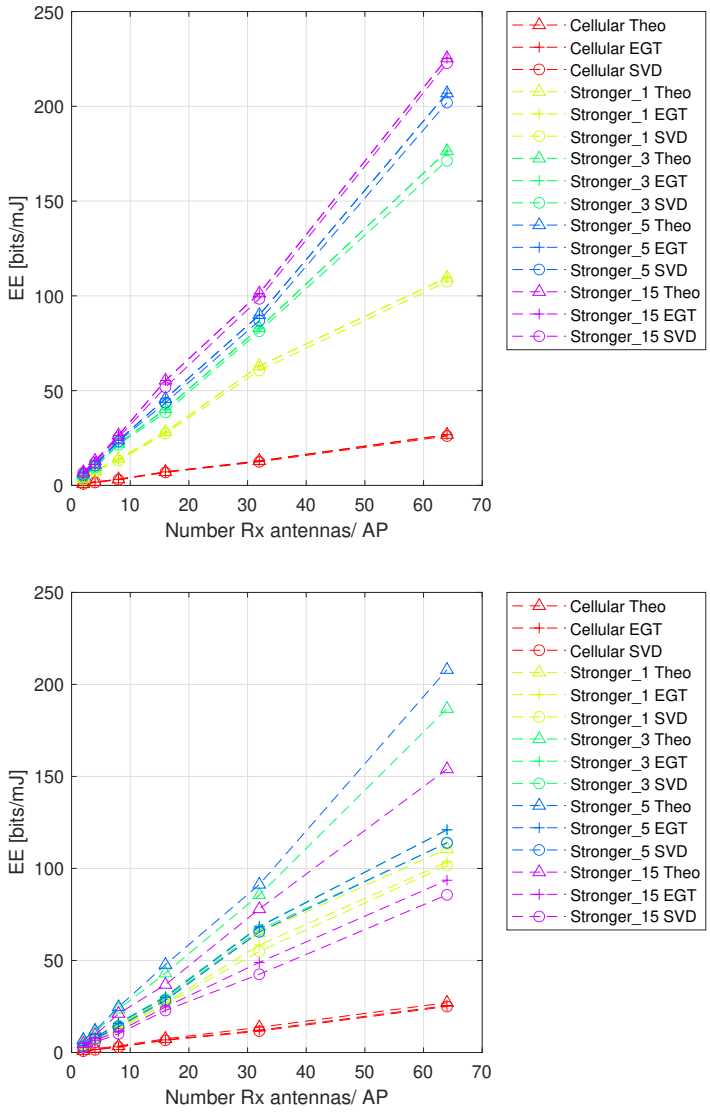


Figure 8: Evaluation of the energy efficiency corresponding to $SE_{50\%}$ = 2.5 bits/s/Hz for EGT and SVD precoding schemes with MRC (top) and EGC (bottom) combiners (Uplink, $N_t = 2$, H-polar only, $N_0 = -88$ dBm/RB), $\alpha_{PA} = 1$, $P_{RU} = P_{DU} = P_{Xhaul} = 0$ (not taken into account).

Like for SE, the practical performance is very close to the theoretical limit with MRC combiner. The optimal configuration is the cooperation between all the possible APs ('Stronger 15') reaching about $220$ bits/mJ (or kb/J). When it comes to EGC, the EE performance gap between theoretical and practical performance is appreciable. The optimal configuration is 'Stronger 5' for both EGT and SVD precoders with about $120$ bits/mJ.

### 3.4 Downlink $N_r = 2$

We first evaluate the theoretical performance based on (14) and (12). The results are presented in Figure 9. The result may look surprising because MRC is known to provide the best performance over Rayleigh channels. However in our scenario, LOS paths prevail[1]. It seems worth noticing that the performance gap increases when AP cooperation is considered.

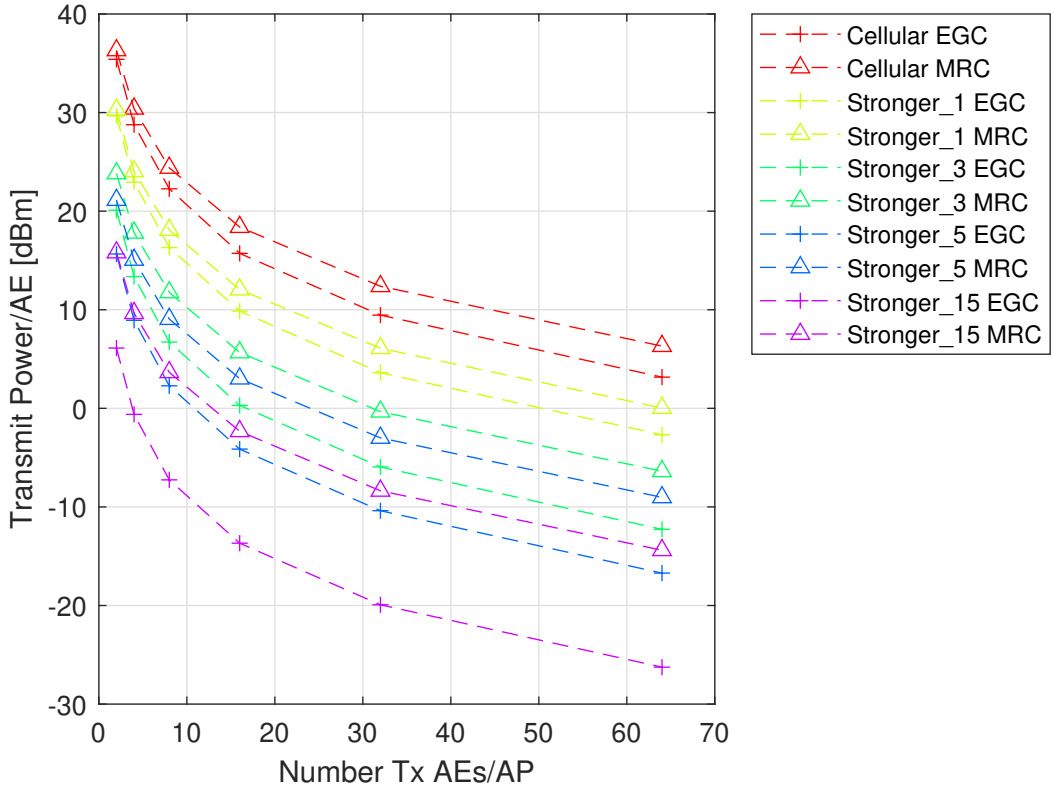


Figure 9: Theoretical bounds of transmitted power per AE required to achieve DL $SE_{50\%}$ = 2.5 bits/s/Hz (Downlink, $N_r = 2$, H-polar only, $N_0 = -88$ dBm/RB)

Figure 10 depicts the results for MRC (top) and EGC (bottom) combiners. As aforementioned, there is no direct solution for EGT precoders when $N_t > 2$ therefore only the SVD precoder will be considered from now on. First of all, one can observe that there is a performance gap between achievable and theoretical performance which enlarges when AP cooperation (and thus number of Tx AEs) increases: more than $10$ dBm with 'Stronger 15' and $64$ AEs/AP ($960$ AEs). For both EGC and MRC combiner, the best scenario remains the full AP cooperation 'Stronger 15'. However, the performance gap is limited when more than $3$ APs cooperate. The difference of performance between the two combiner schemes is limited.

We can now evaluate the EE. We observe with the analysis of the SE, that the required transmit power to satisfy $SE_{50} = 4$ bits/s/Hz may be lower than $-10$ dBm which does not make really sense. That is the reason why, for the EE evaluation, only Tx Power per AE greater or equal than $-10$ dBm will be considered. Figure 11 depicts the results for MRC (top) and EGC (bottom) combiners.

First of all, one can observe that for most scenarios, an optimal number of Tx AEs/AP appear. The more APs cooperate, the lower the optimal number of AEs/AP is. Regarding EGC combiner, the maximum level of EE is

[1]See D1.2

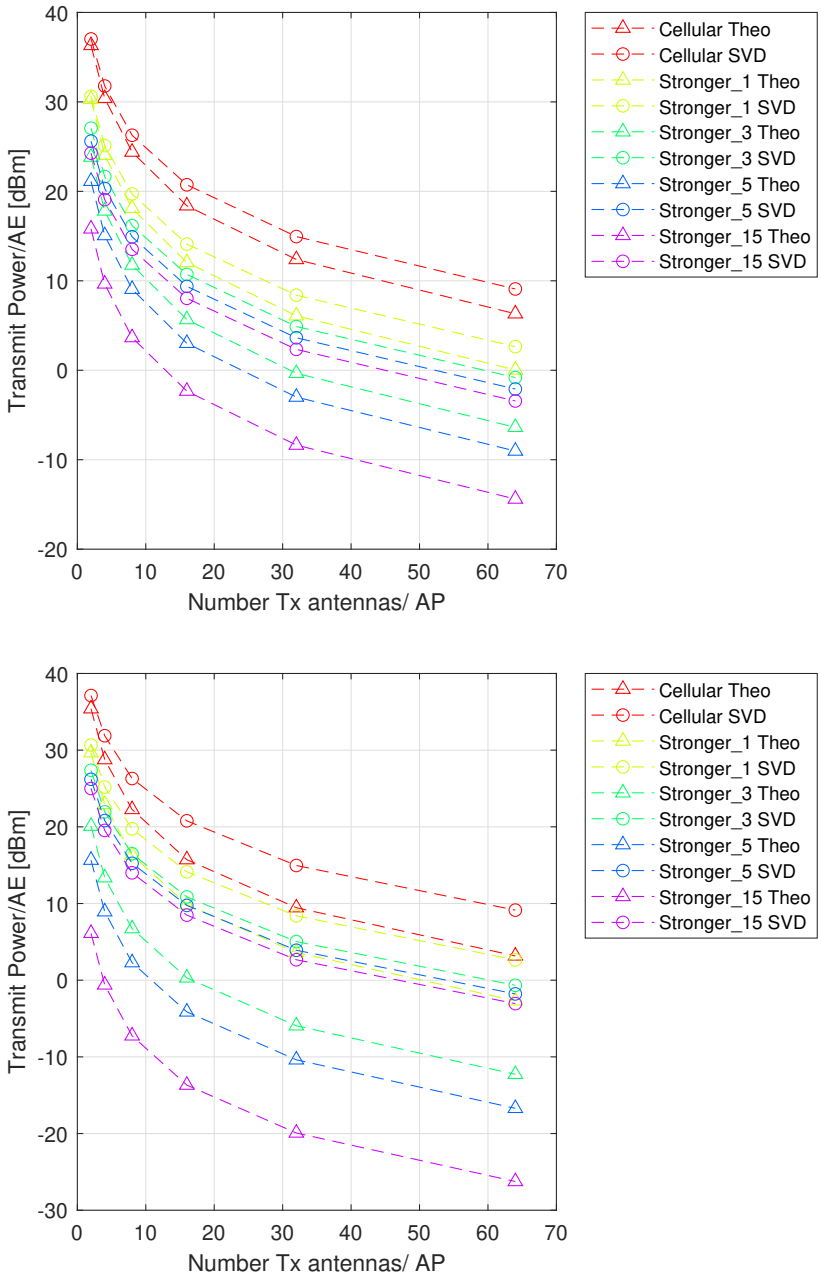


Figure 10: Evaluation of the transmitted power per AE required to achieve DL $SE_{50\%}$ = 2.5 bits/s/Hz for EGT and SVD precoding schemes with MRC (top) and EGC (bottom) combiners (Downlink, $N_r = 2$, H-polar only, $N_0 = -88$ dBm/RB)

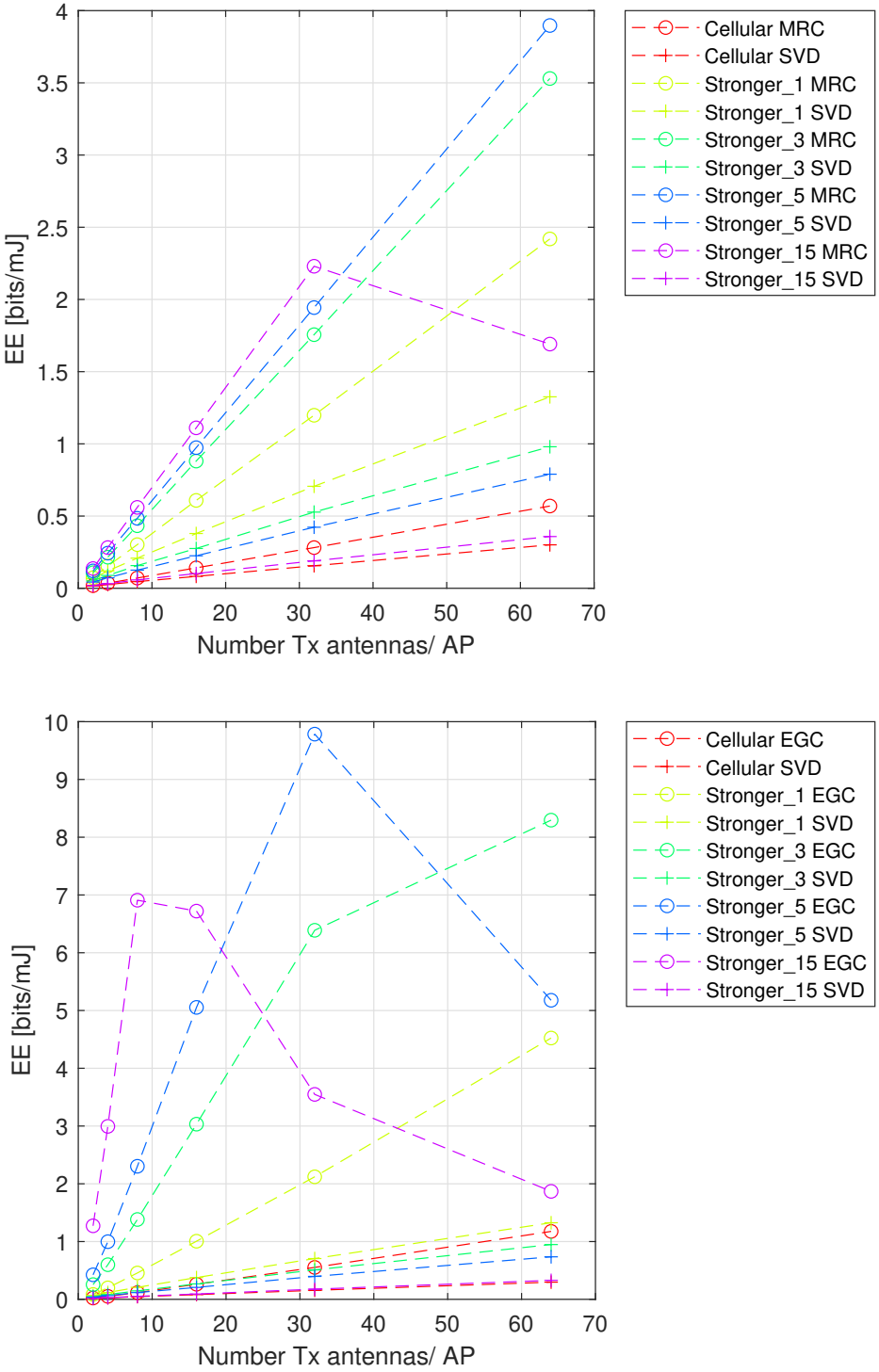


Figure 11: Evaluation of the energy efficiency corresponding to $\mathrm{SE}_{50\%} \geq 2.5$ bits/s/Hz under the power constraint $P \geq -10$ dBm for EGT and SVD precoding schemes with MRC (top) and EGC (bottom) combiners (Downlink, $N_t = 2$, H-polar only)

reached by 'Stronger 5' (*i.e.* AP selection among all the possible APs) with about $10$ bits/mJ for $N_t = 32$. The worst two scenarios are 'Cellular' and 'Stronger 15'. Besides, there is a significant gap between theoretical and practical performance, as already observed with Figure 10. The best practical EE level is also provided with 'Stronger 1' scenarios for $N_t 64$ with about $1$ bits/mJ. When it comes to EGC combiner, the practical performance is similar. It seems also interesting to notice that some curves are not monotonic (mainly theoretical bounds) and admits a maximum value. It is related to the power range that we consider in the study (at least $-10$ dBm per transmit antenna). Indeed, to properly evaluate the EE, the SE results obtained in Figure 10 are bounded to satisfy the power range requirement which leads to the apparition of the maximum EE values in Figure 11. The position and value of those maximums directly depends on the considered power range.

### 3.5 Lesson learnt and perspectives

In the proposed study, the EE is evaluated from the total radiated power. This performance indicator is limited, especially for the uplink scenario (the complexity of the cooperative combining is not taken into account). It is therefore required to derive relevant power consumption models to strengthen our analysis. Besides, the considered transmit power range directly impacts the evaluation of the EE. The values to consider should be carefully chosen.

# 4 Integration plan

The previous section presents a simple scenario based on a coverage measurement combined with an energy consumption measurement. This scenario compares, as fairly as possible, a localized antenna scenario and a distributed antenna scenario.

The integration plan is illustrated on Figure 12. We propose to extend the empty factory scenario by considering, on the one hand, multi-layer single-user and multi-user cases, and on the other hand, link degradations, notably with the use of noisy channel information. Secondly, studies on the use of codebooks will be evaluated. Subsequently, the same studies will be carried out on a factory with furniture.

Finally, we propose to continue investigations into the Paris scenario for mobile broadband applications in a first static version. Work from WP2 can be integrated as well as the modeling of HW impairments. An unified energy consumption model for distributed MIMO networks will be proposed by the partners to integrate fair comparisons of energy consumption between distributed and localized MIMO. In a final step, mobility will be added to the scenarios and the various algorithms will be evaluated.

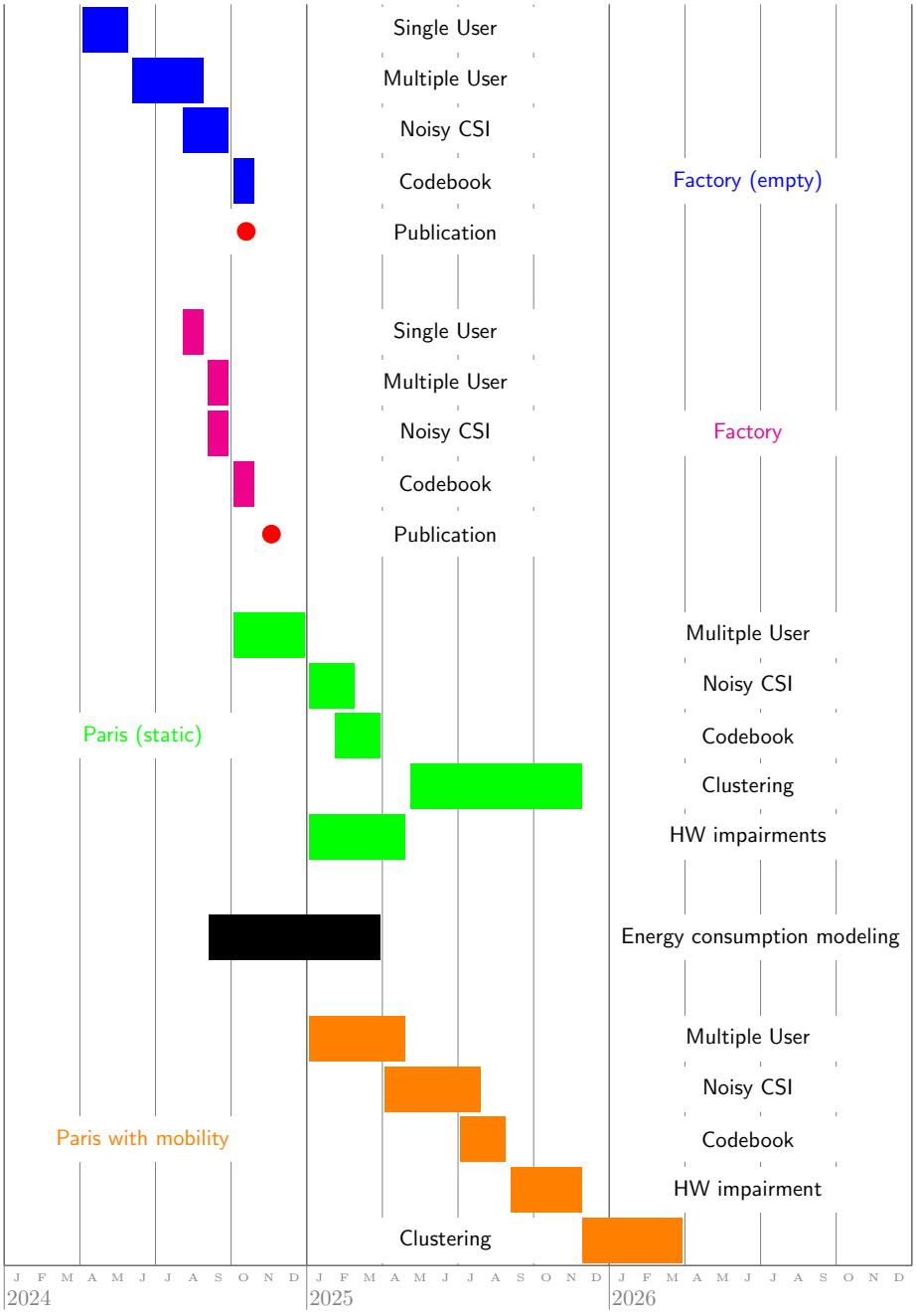


Figure 12: Integration plan

# Appendices

## A Results for emtpy factory scenario, Downlink $N_r = 1$

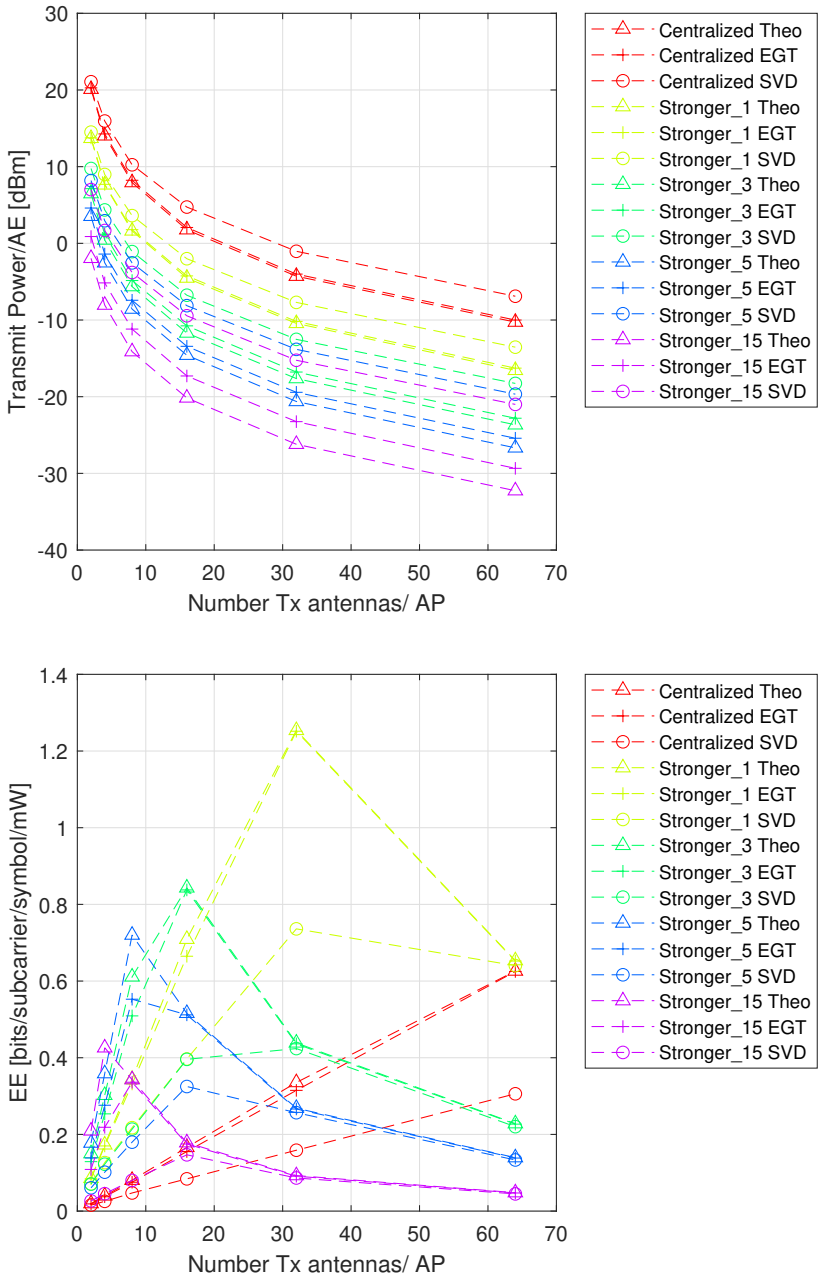


Figure 13: Evaluation of the power required to achieve DL $\text{SE}_{50\%} \geq 4$ bits/s/Hz and corresponding energy efficiency under the power constraint $P \geq -10$ dBm for EGT and SVD precoding schemes with MRC (top) and EGC (bottom) combiners ($N_r = 1$, H-polar only, $N_0 = -88$ dBm/RB)

# B Results for emtpy factory scenario, Uplink $N_t = 1$

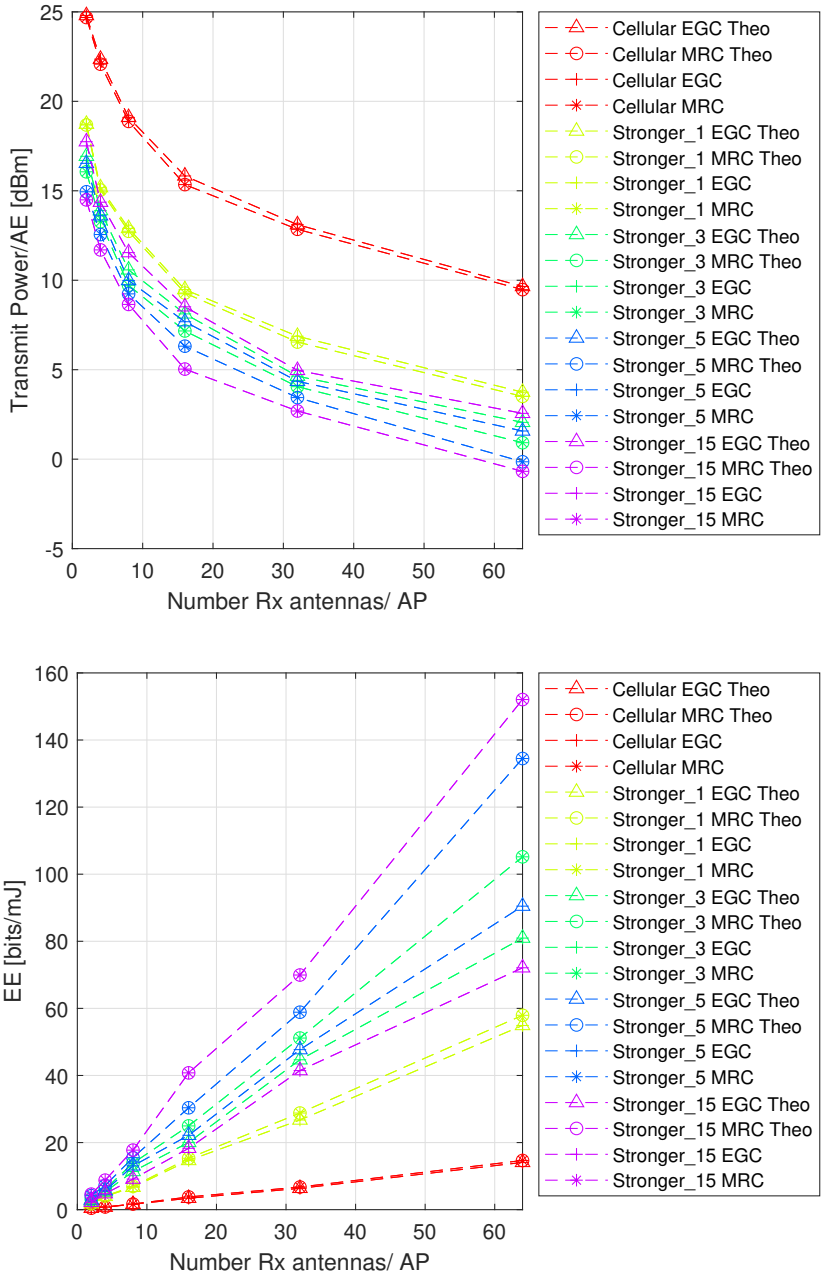


Figure 14: Evaluation of the power required to achieve UL $\text{SE}_{50\%} \geq 4$ bits/s/Hz and corresponding energy efficiency under the power constraint $P \geq -10$ dBm for EGT and SVD precoding schemes with MRC (top) and EGC (bottom) combiners ($N_t = 1$, H-polar only, $N_0 = -88$ dBm/RB)

## References

[1] Emil Björnson, Jakob Hoydis, and Luca Sanguinetti. Massive MIMO networks: Spectral, energy, and hardware efficiency. *Foundations and Trends® in Signal Processing*, 11(3-4):154–655, 2017.

[2] Özlem Tuğfe Demir, Meysam Masoudi, Emil Björnson, and Cicek Cavdar. Cell-free massive mimo in virtualized cran: How to minimize the total network power? In *ICC 2022 - IEEE International Conference on Communications*, pages 159–164, 2022.

[3] D.J. Love and R.W. Heath. Equal gain transmission in multiple-input multiple-output wireless systems. *IEEE Transactions on Communications*, 51(7):1102–1110, 2003.